Theor Chim Acta (1991) 79: 183–190

Theoretica Chimica Acta

Computation of cross sections for the $F + H_2(v = 0, j = 0) \rightarrow FH(v'j) + H$ reaction by the hyperspherical method

J. M. Launay
UPR 261 du CNRS, Observatoire de Paris, F-92195 Meudon, France

Received September 1, 1990/Accepted November 13, 1990

Summary. A quantum mechanical calculation of cross sections for the reaction $F + H_2(v = 0, j = 0) \rightarrow FH(v'j') + H$ has been performed on the T5A semi-empirical potential surface using hyperspherical coordinates. State-to-state integral and differential cross sections converge rapidly with the number of components of the total angular momentum projection onto the axis of least inertia. The $v' = 3$ differential cross section has a forward peak whose magnitude increases with energy whereas the $v' = 2$ differential cross section has a backward maximum, in qualitative agreement with cross-beam experiments. The $v' = 2$ and $v' = 3$ rotational distributions are in rather good agreement with experiment, but not the vibrational branching ratios.

Key words: Hyperspherical coordinates – Cross sections – FH_2 – Quantum dynamics – Chemical reactions

1. Introduction

The recent availability of large memory vector computers has permitted the development of new exact quantum mechanical methods for the determination of cross sections of reactive processes [1]. Much effort has been devoted in the past few years to the $H + H_2 \rightarrow H_2 + H$ [2–5] and $D + H_2 \rightarrow DH + H$ reactions [6–7]. However, it is necessary to test the usefulness of the new methods on less academic systems.

The $F + H_2 \rightarrow FH + H$ reaction, which is important in the design of infrared chemical lasers, has been the subject of very detailed studies by molecular beam techniques [8] and despite intense theoretical work, a quantitative description of all its aspects is not yet in hand [9]. Because this reaction is a highly exoergic one, many more quantum states are populated than in the above mentioned prototype reactions. It is thus a good candidate to test the ability of new theoretical methods to produce converged state-to-state integral and differential reaction cross sections on more complex systems. In this study, we use the semiempirical T5A surface [10], which is currently believed to be the most realistic one for this system.

2. Theory

The nuclear motions in the FHH system can be described with mass-scaled Jacobi coordinates for a generic arrangement λ ($=\alpha, \beta, \gamma$), $\vec{R}_\lambda$ (mass-scaled atom-diatom vector) and $\vec{r}_\lambda$ (mass-scaled internuclear vector of the diatom). Alternatively, we can use a set of hyperspherical coordinates [5, 11] closely related to the Smith–Whitten democratic coordinates [12]. They consist of three Euler angles (denoted collectively by ϖ) which specify the orientation in space of the principal axis frame, the hyperradius $\varrho = \sqrt{R_\lambda^2 + r_\lambda^2}$ which parametrizes the size of the triatomic system, and two angles θ and ϕ_λ which parametrize its shape. The components of $\vec{R}_\lambda$ and $\vec{r}_\lambda$ in the molecular plane Oxz are given by: $Z_\lambda = r_1 \cos\phi_\lambda$, $X_\lambda = -r_2 \sin\phi_\lambda$, $z_\lambda = r_1 \sin\phi_\lambda$, $x_\lambda = r_2 \cos\phi_\lambda$ and the giration radii by $r_1 = \varrho \cos(\theta/2)$, $r_2 = \varrho \sin(\theta/2)$. The angle θ which measures the ratio of the two radii is allowed to vary between 0 and $\pi/2$ and since $r_1 \geqslant r_2$, the body-frame axis z is the axis of least inertia. $\theta = 0$ corresponds to linear configurations and $\theta = \pi/2$ to symmetric top configurations. The range of variation of ϕ_λ is $[0, 2\pi]$. The coordinates associated to a different arrangement ν are the same, except for the angle ϕ which becomes $\phi_\nu = \phi_\lambda - \phi_{\lambda\nu}$ where $\phi_{\lambda\nu}$ is the usual kinematic rotation angle.

Following the diabatic-by-sector method [13], the range of variation of ϱ is divided into sectors $[\varrho_{p-1/2}, \varrho_{p+1/2}]$ centered on ϱ_p. Inside each sector, a partial wave of total angular momentum J, space-fixed component M, parity ε_I and permutation symmetry ε_P for the two hydrogen atoms, is expanded as:

$$\Psi^{JM\varepsilon_I\varepsilon_P}(\varrho\theta\phi\varpi) = \frac{1}{\varrho^{5/2}} \sum_{k\Omega} \varphi_{k\Omega}^{\varepsilon_I\varepsilon_P}(\varrho_p; \theta\phi)\, N_\Omega^{JM\varepsilon_I}(\varpi) f_{k\Omega}^{J\varepsilon_I\varepsilon_P}(\varrho_p; \varrho) \tag{1}$$

In this expression, $N_\Omega^{JM\varepsilon_I}(\varpi)$ is a symmetric top function of definite parity ε_I and Ω is the absolute magnitude of the total angular momentum projection onto the axis of least inertia z. The two-dimensional surface states $\varphi_{k\Omega}^{\varepsilon_I\varepsilon_P}(\varrho_p; \theta\phi)$ which describe the internal θ, ϕ motions in the p-th sector are the eigensolutions of a reference two-dimensional hamiltonian $H^\Omega(\varrho_p)$:

$$H^\Omega(\varrho_p)\varphi_{k\Omega}^{\varepsilon_I\varepsilon_P}(\varrho_p; \theta\phi) = e_{k\Omega}^{\varepsilon_I\varepsilon_P}(\varrho_p)\varphi_{k\Omega}^{\varepsilon_I\varepsilon_P}(\varrho_p; \theta\phi) \tag{2}$$

where:

$$H^\Omega(\varrho_p) = \frac{1}{2\mu\varrho_p^2}\left(-\frac{4}{\sin 2\theta}\frac{\partial}{\partial\theta}\sin 2\theta\frac{\partial}{\partial\theta} - \frac{1}{\cos^2\theta}\frac{\partial^2}{\partial\phi^2} + \frac{4\Omega^2}{\sin^2\theta}\right) + V(\varrho_p; \theta\phi) \tag{3}$$

The fixed-ϱ and fixed-Ω two-dimensional eigenvalue Eq. (2) is solved by a variational expansion over a basis of symmetry-adapted two-dimensional harmonics which generalize the usual spherical harmonics. These harmonics are the solution of Eq. (2) with $V = 0$. For hyperradii $\varrho \geqslant 5a_0$, the surface states φ concentrate into the arrangement valleys, in a small-θ region of configuration space. A contracted basis of θ-localized functions is then built from the harmonics basis, yielding the same results with about 40% less functions at large ϱ. The size of the basis ranges from 400 to 1460 for the FH_2 system, depending on ϱ and Ω values.

The hyperradial functions $f_{k\Omega}^J(\varrho_p; \varrho)$ are the solutions of a set of coupled second-order differential equations with couplings due to the difference between the exact hamiltonian and the reference hamiltonian $H^\Omega(\varrho_p)$. They arise firstly

from the variation of $H^{\Omega}(\varrho)$ inside each sector and secondly from the operator:

$$\mathscr{C}(\varrho) = \frac{1}{2\mu\rho^2}\left(\frac{J_x^2 - J_z^2}{\cos^2\theta/2} + \frac{J_y^2}{\cos^2\theta} - \frac{2i\sin\theta J_y}{\cos^2\theta}\frac{\partial}{\partial\phi}\right) \tag{4}$$

$\mathscr{C}$ is smooth and well behaved at linear ($\theta = 0$) configurations but becomes infinite at symmetric top ($\theta = \pi/2$) configurations which correspond to an isosceles HFH with a bending angle equal to 87.1°. Special care should be taken to handle this singularity when the wavefunction reaches symmetric top configurations [14] but for this system, this happens only for a kinetic energy larger than 1.3 eV, well above the energy range of interest in the present study.

The close coupling equations can be written:

$$\left(-\frac{1}{2\mu}\frac{d^2}{d\varrho^2} + \frac{15}{8\mu\varrho^2} - E\right) f_{k\Omega}^{J\varepsilon_I\varepsilon_P}(\varrho_p;\varrho) + \sum_{k'} H_{kk'}^{\Omega\varepsilon_I\varepsilon_P}(\varrho_p;\varrho) f_{k'\Omega}^{J\varepsilon_I\varepsilon_P}(\varrho_p;\varrho)$$
$$+ \sum_{k'\Omega'} \mathscr{C}_{k\Omega,k'\Omega'}^{J\varepsilon_I\varepsilon_P}(\varrho_p;\varrho) f_{k'\Omega'}^{J\varepsilon_I\varepsilon_P}(\varrho_p;\varrho) = 0 \tag{5}$$

and the coupling matrix elements are given by:

$$H_{kk'}^{\Omega\varepsilon_I\varepsilon_P}(\varrho_p;\varrho) = \langle \varphi_{k\Omega}^{\varepsilon_I\varepsilon_P}(\varrho_p;\theta\phi) | H^{\Omega}(\varrho) | \varphi_{k'\Omega}^{\varepsilon_I\varepsilon_P}(\varrho_p;\theta\phi)\rangle_{\theta\phi} \tag{6a}$$

$$\mathscr{C}_{k\Omega,k'\Omega'}^{J\varepsilon_I\varepsilon_P}(\varrho_p;\varrho) = \langle \varphi_{k\Omega}^{\varepsilon_I\varepsilon_P}(\varrho_p;\theta\phi) N_{\Omega}^{JM\varepsilon_I}(\varpi) | \mathscr{C}(\varrho) | \varphi_{k'\Omega}^{\varepsilon_I\varepsilon_P}(\varrho_p;\theta\phi) N_{\Omega}^{JM\varepsilon_I}(\varpi)\rangle_{\theta\phi\varpi} \tag{6b}$$

Inside each sector, these equations are solved using the de Vogelaere [15] or logarithmic-derivative [16] methods. At the boundary between sectors, the functions and derivatives are transformed from one sector to the next. The sector width is an important parameter of the calculations. If two small, the time needed to compute the surface states is too large. If too large, the flexibility of the surface states basis is reduced and too many are needed to get convergence. In practice, we found that a uniform width of $0.2a_0$ was adequate, in terms of accuracy and efficiency.

The kinetic energy part of the hamiltonian $H^{\Omega}(\varrho)$ has a separable form when expressed as a function of Fock internal coordinates $\omega_\lambda = \tan^{-1}(r_\lambda/R_\lambda)$ and $\eta_\lambda = \cos^{-1}(\hat{R}_\lambda, \hat{r}_\lambda)$ for any arrangement λ [5]. At large ϱ the surface states φ concentrate into the arrangement valleys and the potential becomes independant of the bending angle η_λ. Thus, each surface state φ converges to a separable state $\chi_{\lambda vj}(\varrho;\omega_\lambda)P_j^{\Omega}(\eta_\lambda)$ where P_j^{Ω} is an associated Legendre function and $\chi_{\lambda vj}$ a vibrational function. We are then able to transform the wavefunction of Eq. (1) from the body-fixed hyperspherical representation to a space-fixed Arthurs–Dalgarno representation in Fock hyperspherical coordinates. This transformation is performed in several steps:

— Firstly, we determine for each surface state φ, the set of λvj quantum numbers associated to its behavior at large ϱ.

— Secondly, we transform the wavefunction from the body-fixed principal axis representation to a body-fixed representation where the quantization axis is $\hat{R}_\lambda$, the atom-diatom Jacobi vector of arrangement λ. This transformation involves two-dimensional numerical quadratures. Because in each arrangement λ, the body-fixed axis z is close to $\hat{R}_\lambda$, it is almost unitary.

— Thirdly, a standard body-fixed to space-fixed transformation is performed using analytical methods.

The wavefunction is then matched to asymptotic functions written with Jacobi

coordinates in the Arthurs–Dalgarno representation and the K, S, and T matrices are extracted to produce cross sections. Differential cross sections (DCS) have been computed in the helicity formalism [17].

Our computer code is divided into three stages. The first one concerns the calculation of the φ basis and of the θ, ϕ quadratures which are necessary to build the H^{Ω} and $\mathscr{C}$ couplings. It is independent of the total angular momentum J and of the energy E. The second stage concerns mainly the calculation of integrals over the external ϖ Euler angles present in the $\mathscr{C}$ matrix elements, and of the body-fixed to space-fixed transformation. It depends on J but not on the total energy E and represents a small fraction of the total computer time. The third stage solves the close coupling equations for each J and E value and forms the bulk of the computational effort. It involves mainly matrix multiplications with the de Vogelaere option and matrix inversions with the logarithmic-derivative option. Using highly optimized routines to perform these operations (MINV and MXMA from the SCILIB on a CRAY-2), we found that the logarithmic-derivative method was faster by a factor ranging between 1.5 and 2, for the same accuracy. The convergence of the results can be studied by varying separately the number of k and Ω components in the wavefunction expansion of Eq. (1).

3. Results

State-to-state integral cross sections for the reaction $F + H_2(v = 0, j = 0) \rightarrow FH(v'j') + H$ have already been computed for nine kinetic energies which range from threshold to 5.87 kcal/mol [18]. Partial waves with J ranging from 0 to 31 were considered for each symmetric block $\varepsilon_I = (-1)^J$, $\varepsilon_P = +1$. We found that a basis of 150 surface states φ was adequate to converge $J = 0$ reaction probabilities. Among these states, 14 converge at large ϱ to rovibrational states of the $F + H_2$ arrangement and 136 to rovibrational states of the $FH + H$ arrangement, yielding two closed vibrational manifolds in each arrangement. The $v' = 2$ and 3 reaction probabilities for $J \neq 0$ were converged with a maximum value Ω_m equal to 3. This permitted us to obtain state-to-state integral cross sections with only 552 channels whereas a basis with all Ω components involves 1838 channels. This fast convergence property permits large savings because of the N^3 dependence of computer time with the number N of channels. The total integral reaction cross section obtained in this previous study [18] agrees very well with the value obtained in a recent time-dependent calculation [19].

Here, we are interested in state-to-state differential cross sections and it is not obvious that the same fast Ω-convergence holds for these very detailed quantities. Indeed, we found that $\Omega_m = 3$ is sufficient to converge the $v' = 3$ DCS for all scattering angles ϑ and the $v' = 2$ DCS for $\vartheta > 45°$. $\Omega_m = 10$ is required to converge the $v' = 2$ DCS in the forward direction. This is due to the fact that a truncated Ω basis implies the neglect of $\mathscr{C}$ couplings between the higher Ω components. These couplings increase with total angular momentum J and are large for the high J partial waves which produce forward scattering.

Figure 1 shows the rotationally summed DCS for $E_{\text{kin}} = 2.74$ kcal/mol. They vary smoothly with scattering angle whereas the individual DCS have large amplitude oscillations, mainly for $\vartheta < 90°$. The $v' = 3$ DCS shows a strong and narrow forward peak whose half-width is 10°. Its amplitude increases with increasing energy, whereas the $v' = 2$ DCS has a backward maximum. These features are qualitatively consistent with the crossed-beam experiments [8].

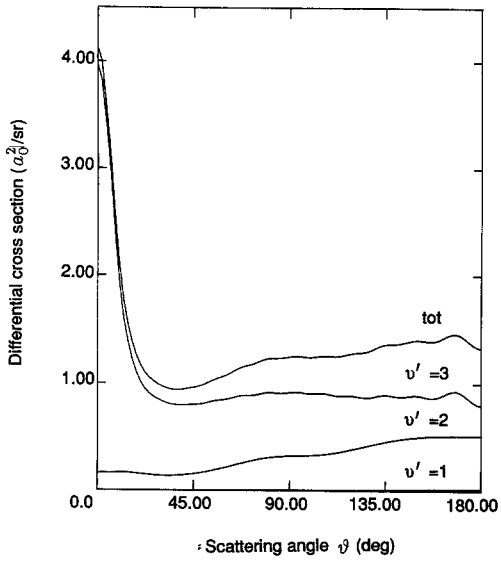

Fig. 1. Rotationally-summed differential cross sections (in a_0^2/sr) for the production of HF(v') at a kinetic energy of 2.74 kcal/mol. The curve labelled "tot" is the total differential reaction cross section

Indeed, the half-width of the experimental $v' = 3$ forward peak is 25°, probably because of the finite angular resolution. The forward to backward DCS ratio for production of HF($v' = 3$) is in semiquantitative agreement with experiment (Table 1). However, no forward $v' = 2$ is detected [8], whereas the present $v' = 2$ forward DCS is small but non negligible.

Figure 2 shows experimental and theoretical rotational distributions for production of FH($v' = 2, 3$). The $v' = 2$ theoretical and experimental distributions look very much the same, although their shape differ slightly. There is a tendency for the theoretical distribution at the highest energy to be too hot and too broad. The $v' = 3$ distributions at $\vartheta = 100°$ are in quantitative agreement but not the distributions in the forward direction.

Table 2 shows that there is a discrepancy in the magnitude of the R_1 and R_3 vibrational branching ratios. R_1 is smaller and R_3 bigger than the corresponding experimental values. This discrepancy is present for all scattering angles (Fig. 1). A reason might be the contribution of $j \neq 0$ initial H_2 states which has not been considered in the present work and indeed, the R_3 theoretical branching ratio is

Table 1. Theoretical and experimental [8] forward to backward differential cross section ratio for the production of FH($v' = 3$) as a function of the kinetic energy E_{kin} in kcal/mol. The experimental results at 1.84 kcal/mol have been obtained with para-H_2 containing more than 80% H_2 in the $j = 0$ state and with normal H_2 at the other energies

E_{kin}	present	Ref. [8]
1.84	2.2	2.5
2.74	5.0	3.7
3.42	6.5	6.1

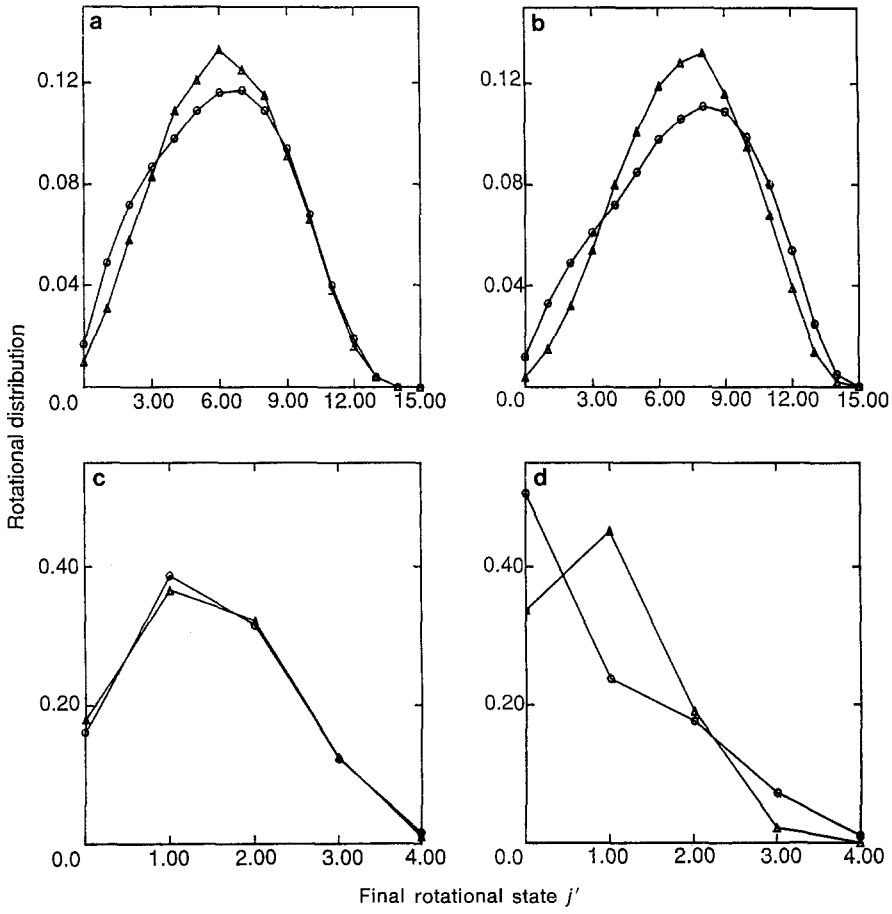

Fig. 2a–d. Rotational populations for production of HF(v') at fixed scattering angle. **a** $v' = 2$, $\vartheta = 140°$, $E_{kin} = 1.84$ kcal/mol; **b** $v' = 2$, $\vartheta = 140°$, $E_{kin} = 2.74$ kcal/mol; **c** $v' = 3$, $\vartheta = 100°$, $E_{kin} = 1.84$ kcal/mol; **d** $v' = 3$, $\vartheta = 0°$, $E_{kin} = 1.84$ kcal/mol. The sum of the populations for each vibrational state is normalized to 1. The present theoretical results are indicated by open circles and the experimental results [8] by upper triangles. The experimental results in (**a**) and (**b**) have been obtained with normal-H_2 and in (**c**) and (**d**) with para-H_2 containing more than 80% H_2 in the $j = 0$ state

Table 2. Theoretical and experimental [8] vibrational branching ratios $R_{v'} = \sigma_{00\to v'}/\sigma_{00\to 2}$, where σ is an integral cross section, for several kinetic energies E_{kin} (kcal/mol). The experimental conditions are as in Table 1

E_{kin}	R_1	R_3	R_1^{exp}	R_3^{exp}
1.84	0.015	3.00	0.20	0.68
2.74	0.021	2.84	0.23	0.53
3.42	0.032	2.44	0.33	0.48

smaller with a $j = 2$ initial state for the $J = 0$ partial wave [20]. However, it remains larger than 1 and it is thus doubtful that this effect can reconcile the theoretical and experimental values. Moreover, the difference between the para-H_2 and normal-H_2 experimental branching ratios is small and the experimental data at 1.84 kcal/mol have been obtained with para-H_2 containing more than 80% H_2 in $j = 0$.

4. Conclusion

We have computed cross sections for the $F + H_2 \rightarrow FH + H$ reaction using a principal axis hyperspherical coordinates formalism. An important aspect of the present formalism is that we can truncate the basis with respect to the body-frame projection Ω. Thus, one difficulty encountered in exact calculations of chemical reactions, namely the large number of magnetic sublevels associated with high j rotational states is in some way circumvented.

As concerns the comparison with experiment, an intriguing aspect of the present calculations is that vibrational branching ratios are not in agreement whereas rotational distributions agree much better. Of course, a more precise comparison requires to include the contribution of $j \neq 0$ initial H_2 states and of the spin-orbit excited fluorine states, especially at the highest collision energy. However, the large discrepancy in vibrational branching ratios may be due to some error in the product region of the potential surface.

The computing time of the present method on this system is a few hours per energy, on a single processor of a CRAY-2 and work on other chemical reactions is in progress. Since more than 95% of the computational effort lies in matrix inversions and multiplications, it may be adapted easily to concurrent supercomputers once efficient library routines are available to perform these operations.

Acknowledgements. The calculations reported in this paper have been performed on a CRAY-2 computer through a grant of the "Conseil Scientifique du Centre de Calcul Vectoriel pour la Recherche" (Ecole Polytechnique, Palaiseau). Financial support from the Groupement de Recherches n°87 "Dynamique des Réactions Moléculaires" is also acknowledged.

References

1. Manolopoulos DE, Clary DC (1989) Annual Reports on the Progress of Chemistry, Section C, 86, chapter 4
2. Mladenovic M, Zhao M, Truhlar DG, Schwenke DW, Sun Y, Kouri DJ (1988) J Phys Chem 92:7035
3. Zhang JZH, Miller WH (1988) Chem Phys Lett 153:465
4. Manolopoulos DE, Wyatt RE (1989) Chem Phys Lett 159:123
5. Launay JM, Le Dourneuf M (1989) Chem Phys Lett 163:178
6. Zhang JZH, Miller WH (1989) J Chem Phys 91:1528
7. Zhao M, Truhlar DG, Schwenke DW, Kouri DJ (1990) J Phys Chem 94:7074
8. Neumark DM, Wodtke AM, Robinson GN, Hayden CC, Lee YT (1985) J Chem Phys 82:3045
9. Levine RD, Bernstein RB (1987) in: Molecular reaction dynamics and chemical reactivity. Oxford University Press
10. Steckler R, Truhlar DG, Garrett BC (1985) J Chem Phys 82:5499

11. Pack RT, Parker GA (1987) J Chem Phys 87:3888
12. Whitten RC, Smith FT (1968) J Math Phys 9:1103
13. Lepetit B, Launay JM, Le Dourneuf M (1986) Chem Phys 106:103
14. Pack RT, Parker GA (1989) J Chem Phys 90:3511
15. de Vogelaere R (1955) J Res Natl Bur Std 54:119
16. Johnson BR (1973) J Chem Phys 13:445; Manolopoulos DE (1986) J Chem Phys 85:6425
17. Goldberger ML, Watson KM (1964) Collison theory. Wiley, New York, p 882
18. Launay JM, Le Dourneuf M (1990) Chem Phys Lett 169:473
19. Neuhauser D, Judson RS, Jaffe RL, Baer M, Kouri DJ (1991) Chem Phys Lett 176:546
20. Yu CH, Kouri DJ, Zhao M, Truhlar DG, Schwenke DW (1989) Intl J Quant Chem Symp 23:45